Respiratory Physiology & Neurobiology 200 (2014) 110–117

Contents lists available at ScienceDirect

Respiratory Physiology & Neurobiology

journal homepage: www.elsevier.com/locate/resphysiol

Ex vivo bubble production from ovine large blood vessels: Size on detachment and evidence of "active spots"

R. Arieli[a,*], A. Marmur[b]

[a] Israel Naval Medical Institute, IDF Medical Corps, Haifa, Israel
[b] Department of Chemical Engineering, Technion – Israel Institute of Technology, Haifa, Israel

ARTICLE INFO

Article history:
Accepted 29 May 2014
Available online 13 June 2014

Keywords:
Decompression bubble size
Hydrophobic surface
Arterial bubbles
Nucleation
Active spot

ABSTRACT

Nanobubbles formed on the hydrophobic silicon wafer were shown to be the source of gas micronuclei from which bubbles evolved during decompression. Bubbles were also formed after decompression on the luminal surface of ovine blood vessels. Four ovine blood vessels: aorta, pulmonary vein, pulmonary artery, and superior vena cava, were compressed to 1013 kPa for 21 h. They were then decompressed, photographed at 1-s intervals, and bubble size was measured on detachment. There were certain spots at which bubbles appeared, either singly or in a cluster. Mean detachment diameter was between 0.7 and 1.0 mm. The finding of active spots at which bubbles nucleate is a new, hitherto unreported observation. It is possible that these are the hydrophobic spots at which bubbles nucleate, stabilise, and later transform into the gas micronuclei that grow into bubbles. The possible neurological effects of these large arterial bubbles should be further explored.

1. Introduction

It has been shown that tiny, flat gas nanobubbles measuring 5–100 nm form spontaneously when a smooth hydrophobic surface is submerged in water containing dissolved gas (Tyrrell and Attard, 2001; Yang et al., 2007). In our previous studies (Arieli and Marmur, 2011, 2013a), these nanobubbles were shown to be the source of gas micronuclei from which bubbles evolved during decompression on smooth hydrophobic, but not hydrophilic, silicon wafers. We further showed (Arieli and Marmur, 2013b) that hydrophobicity on the luminal aspect of ovine large blood vessels was associated with the formation of bubbles after decompression. In our previous investigation, blood vessels were anaerobically separated from the complete heart and lungs, stretched over microscope slides under saline, compressed and decompressed, and then photographed. We surmised that tiny bubbles too small to be detected visually would rise to the saline–air interface. We therefore focused the camera on the saline–air interface to capture bubbles which floated and expanded there. Bubbles were formed in both the venous (right atrium, pulmonary artery, and superior vena cava) and arterial circulation (aorta, pulmonary vein, and left atrium) throughout a period of 80 min following decompression. The formation of bubbles in the arterial circulation after decompression was a new observation. The risk of neurological outcome should be related to the size of the bubble on detachment, especially when this occurs in the arterial circulation. As the bubble becomes larger, its effect on the central nervous system is more severe.

In our previous investigation (Arieli and Marmur, 2013b), we photographed the six vessels in sequence, so that almost 2 min separated sets of photographs from the same vessel. After detachment, bubbles may shift a little sideways from the point of origin, which might introduce a certain measure of confusion. In the present study, therefore, only one blood vessel was compressed and decompressed at a time, and a complete sequence of photographs at 1 s intervals was thus obtained for each blood vessel. Focusing the camera on the tissue–saline interface, as opposed to the saline–air interface, made it possible to determine bubble size on detachment and the exact location of bubble formation.

2. Methods

2.1. Tissue preparation

The complete heart and lungs from seven slaughtered sheep (taken on separate days) were obtained at the abattoir, and on removal intact from the thoracic cavity were immediately immersed in a cooler filled with saline. In the laboratory, under saline and without any exposure to air, samples (area $9.9 \pm 2.4\ cm^2$,

* Corresponding author at: 118 Rakefet, D. N. Misgav, 20175, Israel. Tel.: +972 77 8100825; fax: +972 4 9801210.
E-mail address: rarieli@netvision.net.il (R. Arieli).

http://dx.doi.org/10.1016/j.resp.2014.05.014
1569-9048/

mean ± SD) from the pulmonary artery (PA), pulmonary vein (PV), aorta (AO), and superior vena cava (VC), were gently stretched on microscope slides using metal clips with the luminal aspect exposed. Two slides were placed without exposure to air on the bottom of two Pyrex bowls (diameter 26 cm, height 5 cm) under 2.5 cm saline. The other two slides were kept under saline in the refrigerator for the next day.

2.2. Protocol

The bowls containing the samples were transferred to two different 150-litre hyperbaric chambers (Roberto Galeazzi, La Spezia, Italy). Because the metal clips tended to rust during the exposure, in order to reduce the oxygen pressure the hyperbaric chamber was initially flushed with nitrogen, and the pressure was also elevated using nitrogen. For the maintenance of pressure we used compressed air. Pressure was elevated at a rate of 100 kPa/min to 1013 kPa (90 m sea water, 10 atmospheres absolute), and remained at that pressure overnight (21.1 ± 1.6 h, mean ± SD). Gas saturation close to the blood vessel after 21 h at 1013 kPa was calculated to be 15% of full saturation using equations for transient heat conduction, replacing temperature and heat conductance by concentration and diffusion constants (Eqs. 5.54 and 5.55, Incropera and DeWitt, 1990). The same value was obtained using finite-element computer simulation of gas transfer from a gas phase through the saline. This gas load is similar to the nitrogen load in various diving protocols. In the morning, one of the chambers was decompressed at a rate of 100 kPa/min. The bowl was placed carefully on a nearby table for photography. We immediately started automated photographing (Canon EOS 500d with macro lens 100 mm F/2.8 EF USM), at 1-s intervals for one hour. After the first 30 min of photography, the battery and memory card were replaced and photography resumed for the second 30 min. The 60-min sampling time was chosen because we found previously (Arieli and Marmur, 2013b) that at this point the rate of bubble production began to drop. At the end of the 60 min of photography, the slides with the tissues were removed and photographed against graph paper for later scaling.

The same protocol was followed for the bowl in the second chamber, for the remaining two blood vessel samples from the same animal, and for the samples from each of the other six sheep.

2.3. Analysis

2.3.1. Diameter on detachment

The photographs of each sample were examined in sequence until detachment of a bubble was observed, and the time was noted. The camera was focused on the tissue–saline interface, and when a bubble detached and started floating upwards it went out of focus (Fig. 1). Photographs were also magnified in a search for detachment of bubbles that were too small to be detected when the whole sample was under observation. In most cases the detached bubble was observed before it burst. We therefore reckoned that a 1-s interval between photographs was sufficiently short to capture detachment. Bubble expansion during one second is negligible, so that if one obtains the diameter within 1 s of detachment, this will be a reliable estimate of the diameter on detachment. Bubbles produced near the edges of the tissue were not taken into consideration, and therefore the last 1 mm to the edge of the tissue was not included in the analysis. The area of the blood vessel samples and the diameter of a bubble just before detachment were measured using an image processing programme (Image-Pro-Plus, Media Cybernetics Inc., Bethesda, MD, USA).

2.3.2. Bubble growth rate

When surface tension and other forces related to gas micronuclei stability play a minor role, the diameter of a bubble should be linearly related to time (Appendix 1). Because the gas tension in the saline decreased with time (due to the release of gas to bubbles and the atmosphere), we selected bubbles which detached from the blood vessels between 10 and 20 min after decompression. The diameter was measured backwards in time from detachment in 1-min intervals.

2.3.3. Analysis of active spots

Most of the bubbles were produced at active spots. The diameter of bubbles released from a specific spot and the time sequence of detachment were recorded for further analysis.

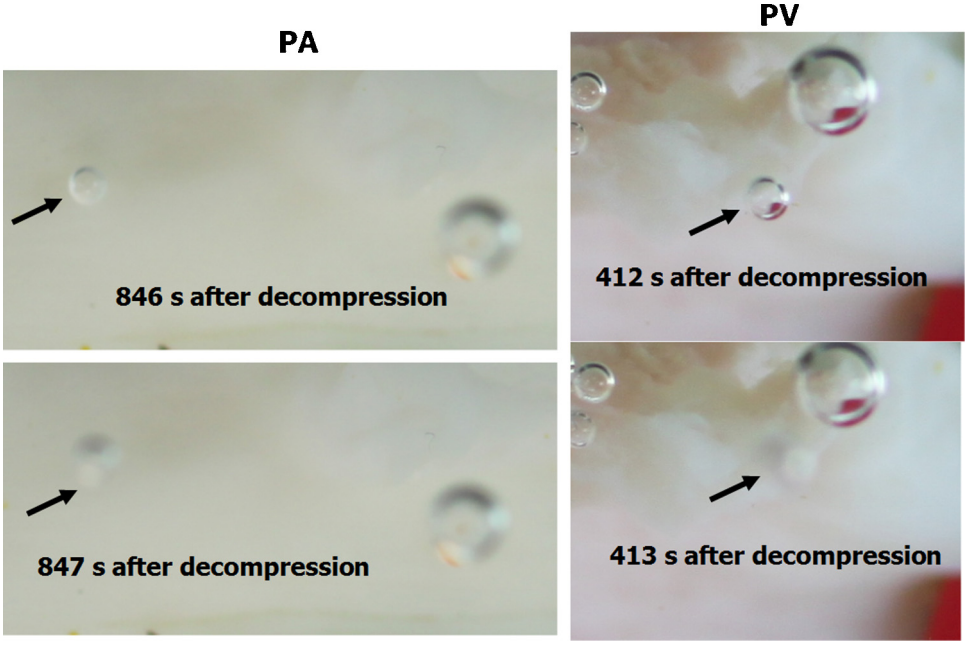

Fig. 1. Detachment of bubbles from the pulmonary artery (PA) and pulmonary vein (PV). After an interval of 1 s, the clearly focused bubble became obscure as it floated upwards.